

# Retrospective Sparse Attention for Efficient Long-Context Generation

Seonghwan Choi\*, Beomseok Kang\*, Dongwon Jo, Jae-Joon Kim

Seoul National University  
{csh3695, beomseok, dongwonjo, kimjaejuon}@snu.ac.kr

## Abstract

Large Language Models (LLMs) are increasingly deployed in long-context tasks such as reasoning, code generation, and multi-turn dialogue. However, inference over extended contexts is bottlenecked by the Key-Value (KV) cache, whose memory footprint grows linearly with sequence length and dominates latency at each decoding step. While recent KV cache compression methods identify and load important tokens, they focus predominantly on input contexts and fail to address the cumulative attention errors that arise during long decoding. In this paper, we introduce RetroAttention, a novel KV cache update technique that retrospectively revises past attention outputs using newly arrived KV entries from subsequent decoding steps. By maintaining a lightweight output cache, RetroAttention enables past queries to efficiently access more relevant context, while incurring minimal latency overhead. This breaks the fixed-attention-output paradigm and allows continual correction of prior approximations. Extensive experiments on long-generation benchmarks show that RetroAttention consistently outperforms state-of-the-art (SOTA) KV compression methods, increasing effective KV exposure by up to  $1.6\times$  and accuracy by up to 21.9%.

## 1 Introduction

With the growing demand for long-context tasks such as reasoning (Jaech et al. 2024; Guo et al. 2025; Comanici et al. 2025), code generation (Chen et al. 2021; Jiang et al. 2024), and multi-turn dialogue (Yi et al. 2024), Large Language Models (LLMs) are increasingly expected to handle extended sequences of input and output. However, supporting such long-context scenarios imposes substantial system-level challenges. A key constraint is the Key-Value (KV) cache, whose memory footprint grows linearly with context length. In practice, the KV cache can occupy several GBs, and fetching it at every decoding step often becomes the main latency bottleneck for inference (Zadouri, Strauss, and Dao 2025; Yuan et al. 2024). As a result, efficient KV cache management has emerged as a critical technique for enabling scalable long-context inference in modern LLMs.

Recent studies have demonstrated that only a small portion of the KV cache plays a critical role in attention computation (Ribar et al. 2023; Zhang et al. 2023; Li et al. 2024). Motivated by this, several KV cache compression

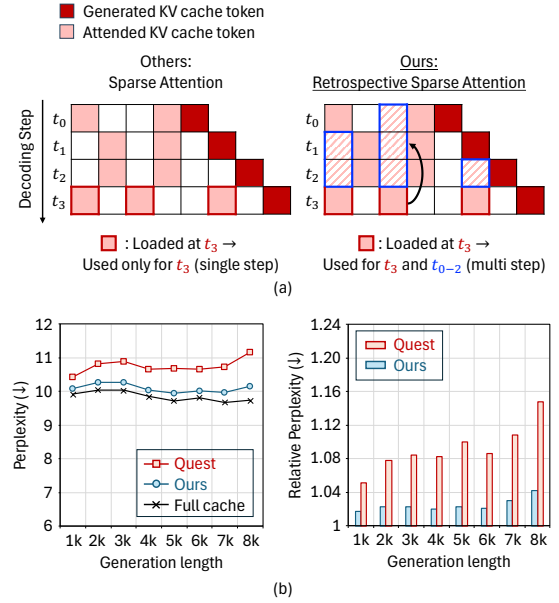


Figure 1: **High-level idea of RetroAttention.** (a) illustrates the key distinction between conventional sparse attention (e.g., Quest) and the proposed Retrospective Sparse Attention. In our approach, KV entries that are currently retrieved ( $t_3$ ) but were unseen in previous decoding steps ( $t_0$ - $t_2$ ) are reused to augment past attention computations. (b) demonstrates the average perplexity depending on the range of generation lengths and relative perplexity between full and compressed KV cache models (right), indicating significant quality degradation as generation continues.

techniques have been proposed to identify and retain important tokens (Liu et al. 2023; Cai et al. 2024; Singhania et al. 2024; Chen et al. 2024b). However, these methods primarily focus on processing long-context *inputs*, rather than *outputs*. Long generation introduces a distinct challenge: errors from approximated attention, due to evicted KV entries, recursively accumulate in the model’s hidden states over extended decoding steps. As illustrated in Fig. 1(b), which evaluates generation quality on PG-19 (Rae et al. 2019), a long-range language modeling benchmark, the performance

\*These authors contributed equally.

gap between models using full and compressed KV cache is initially marginal but becomes substantial as generation progresses. This trend highlights the inherent weakness of existing approaches, which emphasize token selection for the current decoding step while leaving previously decoded tokens unchanged (Yang et al. 2024; Tang et al. 2024; Xiao et al. 2024; Liu et al. 2024a). A naive solution would be to allocate more KV cache budget (*i.e.*, load more KV entries), but doing so increases memory usage and latency, defeating the main purpose of compression. This raises a fundamental research question: How can we mitigate the cumulative attention errors during long generation without increasing the KV cache budget?

In this paper, we propose a novel KV cache *update* technique, called **Retropective Sparse Attention (RetroAttention)**, which enhances approximated attention for past Queries by leveraging future KV entries arriving in subsequent decoding steps (see Fig. 1(a)). To implement this, we allocate a lightweight *output cache* that stores the attention outputs of past Queries. As new KV entries arrive in subsequent steps, we retrospectively compute additional attention outputs for past Queries to update their previous outputs in the cache. This process effectively compensates for errors in the initial attention outputs, thereby improving the quality of KV representations passed to deeper layers. Consequently, each Query benefits from exposure to more KV entries than the static cache budget would allow, without extra KV memory traffic. The key contributions of this work are as follows:

- We introduce **RetroAttention**, a **Retropective Sparse Attention** technique that mitigates cumulative attention errors caused by missed KV cache entries. RetroAttention consistently outperforms SOTA methods on long-generation benchmarks. (Fig. 1, Tabs. 1 and 2)
- We demonstrate that retrospective updates on attention outputs expand the number of KV entries exposed to Queries (*i.e.*, effective budget) by up to 1.6 $\times$ , without increasing actual KV budget. (Fig. 2c)
- Our approach improves accuracy by 5.6% on average (up to 21.9%) compared to SOTA methods in long-generation benchmarks with negligible latency overhead (Figs. 5 and 6).

## 2 Related Works

**Eviction-based KV Cache Compression.** Several KV cache eviction strategies have been proposed to reduce memory usage and accelerate attention computation. Methods such as StreamingLLM (Xiao et al. 2023) retain only the earliest and most recent tokens, while FastGen (Ge et al. 2023) and SnapKV (Li et al. 2024) evicts low-importance tokens after the prefill stage assuming stable attention patterns. Dynamic approaches such as H2O (Zhang et al. 2023), KeyFormer (Adnan et al. 2024), and TOVA (Oren et al. 2024) adaptively determine which tokens to retain based on historical attention statistics. However, all these methods permanently discard selected KV entries, overlooking possible later relevance of evicted tokens—causing cumulative errors or missed dependencies.

**Non-eviction KV Cache Compression.** Non-eviction methods preserve the full KV cache but reduce computation by sparsely loading only relevant tokens per decoding step, allowing revisitation of previously irrelevant entries. Pioneering works, Quest (Tang et al. 2024) and ArkVale (Chen et al. 2024a) identify top- $k$  relevant pages of KV cache (Kwon et al. 2023) via similarity between Queries and page-level summaries. InfLLM (Xiao et al. 2024), Squeeze-dAttention (Hooper et al. 2024), and ClusterKV (Liu et al. 2024b) use representative or centroid Key vectors to generate these summaries. Other methods such as RetrievalAttention (Liu et al. 2024a) and TokenSelect (Wu et al. 2024) dynamically select relevant cache subsets at token granularity. While effective for long-context inputs, these approaches still overlook cumulative attention errors during generation.

**KV Cache Compression for Long Generation.** Few studies address KV cache compression for long generation. Song et al. (2025) exploit the semantic sparsity of reasoning traces by periodically evicting low-importance entries, but may inherit limitations common to eviction-based methods, especially under evolving attention patterns. Concurrent with our work, Sun et al. (2025) raise similar concern about the cumulative errors caused by sparse attention and propose periodically refreshing previous attention outputs using dense attention (*i.e.*, full KV cache). However, this incurs significant computational overhead due to repeated dense attention, in contrast to our contributions—reducing the errors without additional KV cache budget.

## 3 Proposed Approach

### 3.1 Background

**Dynamic Sparse Attention.** RetroAttention adopts Quest’s KV cache selection strategy (Tang et al. 2024) to address evolving importance of KV cache pages during decoding. Quest abstracts each KV cache page into  $K_{\min}$  and  $K_{\max}$ , the element-wise minima and maxima of Key vectors within a page, which highlight extreme feature values. The importance of the  $j$ -th cache page to a given Query is then estimated as:

$$\text{score}_j(Q) = \sum_i \max(Q_i K_{\min,i}^j, Q_i K_{\max,i}^j) \quad (1)$$

where  $i$  indexes the feature dimensions. This can be computed without loading full pages and enables efficient top- $k$  selection of relevant pages at each decoding step.

This approach features that unselected KV entries are not permanently discarded—available for future retrieval if they become relevant. While Quest emphasizes the Query-dependent variability of optimal KV entries, we shift the focus to their *reusability*, using currently loaded entries to retrospectively refine past attention outputs.

### 3.2 Motivational Study

We explore whether the loaded KV entries can be further exploited beyond computing attention for the current Query—specifically, by incorporating KV entries that were

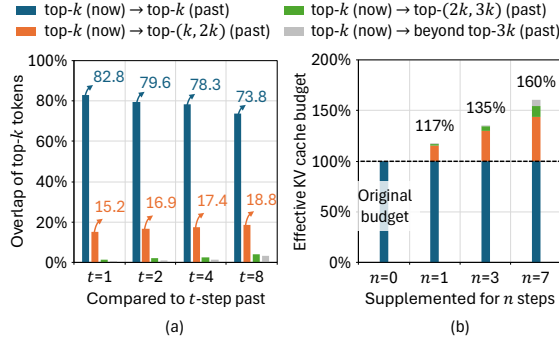


Figure 2: **Long-generation accuracy analysis.** (a) presents the semantic correlation of the current top- $k$  KV entries in the  $t$ -step prior decoding, categorized into different top- $k$  intervals, demonstrating how often current important tokens would have been important in the past. (b) analyzes the effective KV cache budget (*i.e.*, total KV entries exposed to a given Query) when supplemented with entries from  $n$  future decoding steps. Note that this growth may not scale linearly to  $n$ , as supplemented KV entries can be duplicated across updates. Results are experimented with LLAMA3.1-8B-INSTRUCT and GSM8K in LONGGENBENCH.

previously not used during their original attention computation (see Fig. 1(a)). This idea introduces two critical questions: (1) Are the currently loaded KV entries actually useful for improving the attention outputs of past Queries? and (2) How much informational benefit can we expect from leveraging such retrospective refinement?

**Usefulness of Loaded KV Entries for Past Queries.** Sequential tokens often exhibit strong semantic correlations (Dai et al. 2024; Wu et al. 2024), suggesting that KV entries retrieved for the current Query may also be informative for nearby past Queries. To evaluate this, we compute the rank of currently loaded KV entries in past Queries. As shown in Fig. 2(a), about 70–80% of current KV entries were previously within the top- $k$  set (navy bar), while 20–30% were not selected at all. Notably, the second-largest group—about 15–20%—are ranked within the next- $k$  range (orange bar), implying that they are still highly relevant yet were omitted in the past. This highlights the potential of currently loaded KV entries to supplement semantically meaningful but ignored content in the original top- $k$  selection.

**Informational Benefit of Retrospective Updates.** Retrospective updates enable past Queries to access KV entries beyond their original top- $k$  set. As decoding progresses, each past attention can be revised multiple times in subsequent decoding steps, leading to a cumulative expansion of supplemented KV entries. To quantify the total set of KV entries exposed to a Query over time—referred to as the *effective KV cache budget*—we count how many KV entries loaded by future Queries were previously unseen by a given Query (Fig. 2(b)). The effective budget is computed as the union of all KV entries seen by a Query, excluding duplicates. Even with a single future Query ( $n=1$ ), where each

attention updates only its immediate predecessor, the effective budget increases by  $1.17\times$ —a non-trivial gain. As more future Queries supplement, the effective budget continues to grow, reaching up to  $1.60\times$  at  $n=7$ . Importantly, this benefit is achieved without increasing the actual KV cache budget.

These findings motivate our strategy of applying retrospective updates across subsequent multiple Queries: by leveraging each Query’s retrieved KV entries to revise adjacent past attention outputs, we can improve contextual completeness at minimal computational and bandwidth cost.

### 3.3 Retrospective Attention Output Update

Building on insights from our motivational study, we hypothesize that currently loaded KV entries can effectively compensate for attention errors made in earlier steps. These errors stem from the lack of relevant Keys and Values in the attention output ( $O$ ) computation. To correct this, our objective is to revise the previously computed  $O$  vector in a retrospective manner. We introduce two key components to implement this idea: (1) supplementary attention output and (2) attention output cache. Fig. 3 provides an overview of the retrospective attention update process.

**Supplementary Attention Output.** As illustrated in Steps 2 and 3 of Fig. 3, RetroAttention computes attention outputs not only for the current decoding step but also retrospectively for previous steps. For the current step, attention is computed using sparse attention methods *e.g.*, Quest, yielding the output  $O_{\text{org},t}$  (blue box). For past steps, RetroAttention computes attention between previous Queries and the currently loaded—but previously unseen—KV entries, producing  $O_{\text{sup},t}$  (yellow box). We refer to this additional attention output as the *supplementary attention output*. While omitted in the figure, we maintain a mask that tracks the most recent decoding step in which each KV page was loaded, allowing us to identify previously unseen entries. Formally, the attention outputs are defined as follows:

$$O_{\text{org},t} = \frac{\sum_{j \in S_t} \sum_{l \in \text{Page}_j} e^{Q_t K_l^\top / \sqrt{d}} V_l}{\sum_{i \in S_t} \sum_{l \in \text{Page}_i} e^{Q_t K_l^\top / \sqrt{d}}} \quad (2)$$

$$O_{\text{sup},t}^{t+s} = \frac{\sum_{j \in S_{t+s} \setminus \bigcup_{m=t}^{t+s-1} S_m} \sum_{l \in \text{Page}_j} e^{Q_t K_l^\top / \sqrt{d}} V_l}{\sum_{i \in S_{t+s} \setminus \bigcup_{m=t}^{t+s-1} S_m} \sum_{l \in \text{Page}_i} e^{Q_t K_l^\top / \sqrt{d}}} \quad (3)$$

where  $Q_t$  is the  $t$ -th Query vector,  $S_t$  denotes the set of top- $k$  KV cache page indices loaded by  $Q_t$ , and  $\text{Page}_i$  is the set of token indices in  $i$ -th page.  $O_{\text{sup},t}^{t+s}$  refers to supplementary output generated at the  $t+s$ -th decoding step ( $0 < s < w$ ) for  $Q_t$ . Note that supplementation is not limited to adjacent steps; rather, it is applied across multiple past Queries within a retrospective window  $w$ , as described in Fig. 3.

By combining  $O_{\text{org},t}$  and  $O_{\text{sup},t}^{t+s}$  for all  $s$ , we can extend the attention computation for the past Query beyond its original KV cache budget. Accordingly, our goal is to update

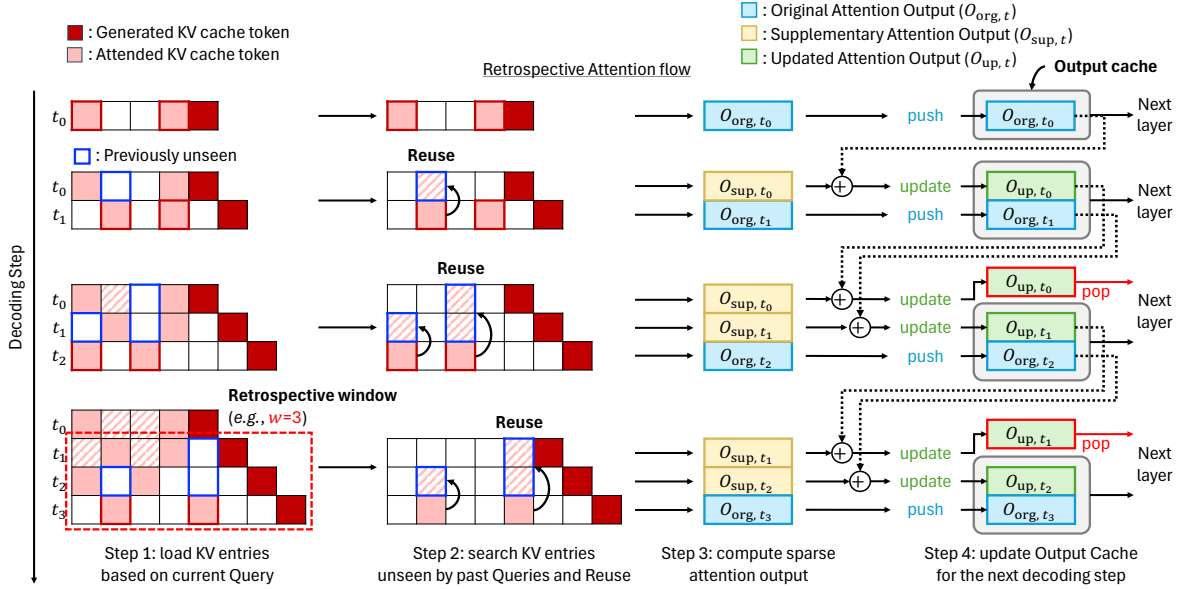


Figure 3: **Retrospective attention output update.** Overview of RetroAttention across three decoding steps, illustrating how previously unseen KV entries are retrospectively reused to refine past attention outputs via supplementary computation and output cache updates. This illustration assumes a retrospective window size of  $w=3$ .

$O_{\text{org},t}$  to  $\text{softmax}(Q_t K^\top / \sqrt{d})V$ , computed over  $K, V$  in  $\text{Page}_i$  where  $i \in \cup_{0 \leq s < w} S_{t+s}$ .

Inspired by the aggregation of partial attention results in FlashAttention (Dao et al. 2022), the softmax equation can be rewritten to a linear combination of the original and supplementary attention outputs (see details in Appendix A), which we refer to as  $O_{\text{up},t}$ . This allows us to *update* earlier outputs using newly available KV entries, efficiently correcting their errors.

**Attention Output Cache.** Retrospective updates require access to the previous attention outputs of past Queries, which are typically discarded after their decoding steps. Recomputing these outputs would necessitate reloading the top- $k$  KV pages for each past Query, increasing the required KV cache budget in proportion to the retrospective window size, which is undesirable. To avoid this, we introduce an *attention output cache*, which stores multiple attention outputs (current and previous steps). This cache consumes marginal memory, with a size of  $(w-1, B, L, D)$ —corresponding to the restrospective window size  $w$ , batch size  $B$ , number of layers  $L$ , and hidden dimension  $D$ —and is independent of the generation length, unlike KV cache.

The cache operates via three actions, as depicted in Step 4 of Fig. 3: (1) Push: attention output computed at each decoding step is stored in the cache. (2) Update: when supplementary attention outputs become available, the cached outputs, either the original  $O_{\text{org}}$  or previously updated  $O_{\text{up}}$ , are reused to compute revised outputs via weighted combination. This allows both initial updates ( $O_{\text{org}} \rightarrow O_{\text{up}}$ ) and re-updates ( $O_{\text{up}} \rightarrow O_{\text{up}}$ ). (3) Pop: when the number of cached entries exceeds the window size, the oldest entry is evicted.

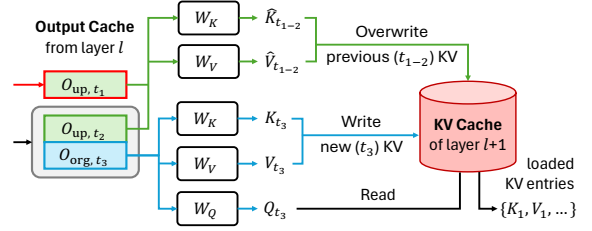


Figure 4: **Retrospective KV cache update.** Output cache from the previous layer provides multiple embeddings ( $t_{1-3}$ ) to the current layer. The most recent output ( $t_3$ ) is used to generate new KV entries, while earlier outputs ( $t_{1-2}$ ) produce updated KV entries that overwrite previous ones in the current layer’s KV cache. Feed-forward and normalization layers are omitted.

### 3.4 Retrospective KV Cache Update

The above components describe how attention is updated within a single layer. However, they do not fully describe how refined past outputs propagate across layers and influence final generation. Here, we show how retrospective updates modify the KV cache in deeper layers.

**Influences on Deeper Layers.** As shown in Fig. 4, the output cache from the layer  $l$  provides multiple embeddings (e.g.,  $O_{\text{up},t_{1-2}}(l)$  and  $O_{\text{org},t_3}(l)$ ) to the layer  $l+1$ . For the most recent step  $t_3$ , the layer  $l+1$  has not yet been computed. Thus, the projection layers generate Query  $Q_{t_3}(l+1)$ , Key  $K_{t_3}(l+1)$ , and Value  $V_{t_3}(l+1)$  for the first time. These Key and Value are newly appended to the KV cache (blue line). For previous steps  $t_{1-2}$ , we re-embed  $O_{\text{up},t_{1-2}}(l)$  to

compute new Queries  $\hat{Q}_{t_{1-2}}(l+1)$ , Keys  $\hat{K}_{t_{1-2}}(l+1)$ , and Values  $\hat{V}_{t_{1-2}}(l+1)$ . These differ from the original KV entries generated using  $O_{\text{org}, t_{1-2}}(l)$  (i.e.,  $K_{t_{1-2}}(l+1)$  and  $V_{t_{1-2}}(l+1)$ ), which are now outdated. Hence, we overwrite the previous KV entries with updated ones:  $K_{t_{1-2}}(l+1) \rightarrow \hat{K}_{t_{1-2}}(l+1)$  and  $V_{t_{1-2}}(l+1) \rightarrow \hat{V}_{t_{1-2}}(l+1)$  (green line). As a result, future decoding steps that access these KV entries benefit from higher-quality attention states. RetroAttention thus improves the KV cache itself, allowing downstream layers to operate on refined representations.

### 3.5 Overhead Analysis

Conventional attention operations heavily rely on GEMV (General Matrix-Vector multiplication) during decoding, leading to extremely low PE (Processing Element) utilization. We strategically design RetroAttention to exploit this idle parallelism for retrospectively updating past attention outputs and KV entries, using currently loaded KV entries. As a result, the additional computation in RetroAttention incurs only marginal overhead in memory and latency. To support this claim, we provide a per-layer overhead analysis.

**RetroAttention’s Overhead in Attention Layers.** We analyze RetroAttention’s Arithmetic Intensity (AI)—the ratio of FLOPs to bytes accessed from main memory—to show it operates in a memory-bound regime.

Its FLOPs scale with the retrospective window size  $w$ , number of loaded KV pages  $k_{\text{page}}$ , Query heads  $h_q$ , tokens per page  $P$ , and head dimension  $d$ , and is estimated as  $4w k_{\text{page}} h_q P d$  in FP16. This involves four types of memory access: (1) loading  $2w h_q d$  bytes for Query vectors, (2) loading  $4 k_{\text{page}} h_k P d$  bytes for KV cache pages, (3) accessing  $4 h_k k_{\text{page}}$  bytes for a mask tracking KV page usage, and (4) writing  $2w h_q d$  bytes for the output.

$$\text{AI}_{\text{attention}} = \frac{w k_{\text{page}} h_q P d}{w h_q d + k_{\text{page}} h_k P d + h_k k_{\text{page}}} \quad (4)$$

As  $w h_q \ll k_{\text{page}} P$  and  $h_k \ll P d$ , Eq. (4) simplifies approximately to  $w h_q / h_k$ . Given that modern GPUs typically shift to compute-bound above AI values of 200-400 (Zhu et al. 2025), RetroAttention remains memory-bound for moderate window sizes (e.g.,  $w < 100$ ), making latency primarily memory-driven. That is, we can quantify the latency overhead by comparing memory traffic. Baseline (e.g., Quest) sparse attention loads  $h_q d$  for Queries and  $k_{\text{page}} h_k P d$  for KV cache pages. The memory traffic ratio is:

$$\frac{\text{Our Mem I/O}}{\text{Baseline Mem I/O}} = \frac{w h_q d + k_{\text{page}} h_k P d + h_k k_{\text{page}}}{h_q d + k_{\text{page}} h_k P d} \quad (5)$$

As KV loads ( $k_{\text{page}} h_k P d$ ) dominate both numerator and denominator, our memory communication overhead is negligible (i.e., the ratio stays near 1 for moderate  $w$ ). This indicates marginal latency overhead from RetroAttention.

**RetroAttention’s Overhead in Linear Layers.** Linear layers in RetroAttention are accompanied by  $w$  embeddings, processing input matrices of shape  $w b \times D$ , where  $b$  is a batch

size and  $D$  is the feature dimension. The AI of RetroAttention’s linear layers is as follows:

$$\text{AI}_{\text{linear}} = \frac{w b D_{\text{in}} D_{\text{out}}}{w b (D_{\text{in}} + D_{\text{out}}) + D_{\text{in}} D_{\text{out}}}, \quad (6)$$

where  $D_{\text{in}}$  and  $D_{\text{out}}$  are the input and output dimensions of a linear layer. They remain memory-bound as long as  $w b$  is below a few hundred, with overhead scaling with memory traffic rather than computation. Our method increases memory traffic (denominator in Eq. 6) in the first term by  $w$  times, but the second term ( $D_{\text{in}} D_{\text{out}}$ ) dominates, yielding only minor latency overhead. See Appendix B for details.

## 4 Experimental Results

**Datasets and Implementation Details.** Our main benchmark is LONGGENBENCH (Liu et al. 2024c) in which multiple reasoning tasks are sequentially concatenated into a single input prompt (details in Appendix D). Such prompt scheme is applied to CSQA (Talmor et al. 2019), MMLU (Hendrycks et al. 2021), and GSM8K (Cobbe et al. 2021) datasets, and a parameter  $n$  determines the number of questions in a prompt. Reasoning-intensive benchmarks such as AIME 2024, GPQA-DIAMOND (Rein et al. 2024), and LIVECODEBENCH (Jain et al. 2024) are included. We also include PG-19 (Rae et al. 2019) benchmark to estimate long-sequence language modeling performance using perplexity. All experiments are performed with LLAMA-3.1-8B-INSTRUCT but with DEEPSEEK-R1-DISTILL-LLAMA-8B for the reasoning-intensive tasks. Our implementation adopts Quest’s page selector (Tang et al. 2024) and is built on FlashInfer (Ye et al. 2025), a highly optimized implementation of attention.

**Baselines.** We compare three recent KV-cache compression methods—StreamingLLM (Xiao et al. 2023), TOVA (Wu et al. 2024), and Quest (Tang et al. 2024)—each employing a distinct token-selection strategy. StreamingLLM and TOVA are both eviction-based techniques. StreamingLLM relies on a static cache window whereas TOVA adaptively retains KV entries based on heuristic token significance estimation. We include these methods as they have not been rigorously evaluated under long-generation scenarios. Our primary baseline is Quest, a SOTA non-eviction method that selects a subset of tokens through Query-aware, paged sparse attention.

### 4.1 Comparison with SOTA methods

We compare the proposed method with the baselines in long-generation GSM8K, MMLU, and CSQA datasets, provided in LONGGENBENCH. Tab. 1 summarizes accuracy results on the three datasets as the number of questions concatenated in a prompt ( $n$ ) increases. Overall input and output tokens range between about 1.3k-5.7k and 0.6k-4.2k, respectively. A higher  $n$  indicates longer input and output lengths. See data statistics in Appendix D.

**Accuracy Analysis for Eviction-based Baselines.** StreamingLLM and TOVA fail across all three datasets, even when  $n$  is small. This suggests that their failure stems



Table 1: **Comparison with SOTA methods.** Accuracy results on GSM8K, MMLU and CSQA in LONGGENBENCH with three  $n$  (i.e., the number of questions in a prompt) values are summarized. All methods use relative KV cache budget of 0.15, which dynamically changes the budget to context length  $\times$  0.15 as decoding continues, with the minimum budget of 256 tokens. We set the retrospective window size ( $w$ ) to 2.

Method / Benchmark	$n$ -question GSM8K ( $\uparrow$ )				$n$ -question MMLU ( $\uparrow$ )				$n$ -question CSQA ( $\uparrow$ )			
	15	30	45	Mean Acc.	15	30	45	Mean Acc.	15	30	45	Mean Acc.
Full Attention	66.7	60.8	58.0	61.8	62.5	58.7	57.1	59.4	73.5	74.1	71.9	73.2
StreamingLLM	0.0	0.0	0.0	0.0	1.2	2.1	2.5	1.9	0.8	1.1	4.0	2.0
TOVA	0.2	0.3	0.2	0.2	9.7	8.7	9.4	9.3	6.7	6.3	11.1	8.1
Quest	<u>58.2</u>	<u>50.9</u>	<u>48.6</u>	<u>52.6</u>	<u>58.8</u>	<u>54.9</u>	<u>50.6</u>	<u>54.8</u>	<b>70.9</b>	<u>53.5</u>	<u>46.1</u>	<u>56.8</u>
<b>RetroAttention (Ours)</b>	<b>61.3</b>	<b>52.6</b>	<b>55.4</b>	<b>56.5</b>	<b>59.3</b>	<b>55.4</b>	<b>51.2</b>	<b>55.3</b>	<u>68.8</u>	<b>59.1</b>	<b>53.0</b>	<b>60.3</b>
$\Delta$ Ours - Quest	+3.1	+1.7	+6.8	+3.9	+0.5	+0.5	+0.6	+0.5	-2.1	+5.7	+6.9	+3.5

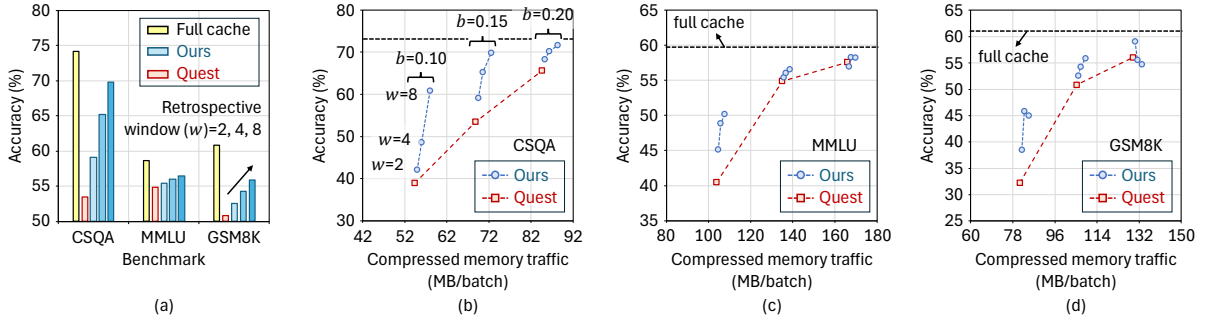


Figure 5: **Ablation studies.** (a) Comparison between full cache (no compression), Quest, and ours in LONGGENBENCH with three retrospective window sizes. We set the relative budget to 0.15. (b)–(d) present the trade-off between the attention memory traffic and accuracy with three relative budget ( $b$ ) values in CSQA, MMLU, and GSM8K, respectively. We set  $n$  to 30.

from an inherent limitation of the methods in sequential question-answer scenarios, rather than a challenge specific to *long* generation. Both approaches permanently evict KV cache entries, meaning that tokens relevant to later questions may be discarded during earlier decoding steps and can never be recovered. Thus, the model is unable to attend to upcoming content when needed, revealing a critical weakness of eviction-based strategies.

**Accuracy Analysis for Non-eviction Baseline.** While exhibiting higher accuracy, Quest also experiences a noticeable accuracy drop at high  $n$  (see Tab. 1). In particular, the performance gap between full cache and Quest becomes larger as  $n$  grows (e.g., -2.6%p, -20.6%p, and -25.8%p in CSQA), implying the cumulative errors caused by approximated attention. In contrast, our approach is robust to such performance degradation, consistently outperforming Quest in nearly all configurations. The performance gain of RetroAttention over Quest is particularly large with higher  $n$  (e.g., 6.8%p in GSM8K, 6.9%p in CSQA), highlighting the effectiveness of our retrospective updates.

We also compare our method against Quest with larger retrospective window sizes ( $w$ ). Fig. 5(a) shows accuracy results of full cache, Quest, and RetroAttention under the three window sizes ( $w \in \{2, 4, 8\}$ ). As  $w$  increases, RetroAttention approaches the performance of the full cache baseline more closely across all benchmarks.

**Memory Analysis.** Increasing the KV budget is a straightforward way to improve the accuracy at the cost of additional memory traffic. Our method redesigns such trade-off through retrospective updates. Figs. 5(b)–(d) show comprehensive comparisons between Quest and ours with three relative KV cache budgets ( $b$ ). The relative budget adaptively changes the amount of KV entries to be loaded by context length  $\times b$ . As shown in the figure, RetroAttention yields significant accuracy gains over Quest at a given budget with negligible memory traffic overhead of 3.0% in CSQA, 1.6% in MMLU, and 2.0% in GSM8K on average.

**End-to-End Latency.** Fig. 6(a) presents the average end-to-end latency per decoding step for the full-cache baseline, Quest, and ours (setup details in Appendix D). RetroAttention consistently outperforms the full-cache baseline and remains at similar latency with Quest across all context lengths. The additional latency of RetroAttention over Quest is minimal, less than 1ms per token for  $w=2$  and around 2ms for  $w=8$ . Importantly, this overhead remains effectively constant regardless of context length or retrieved cache size, aligned with our theoretical analysis in Sec. 3.5, which attributes the overhead primarily to additional memory I/O.

**Kernel-level Attention Latency.** Fig. 6(b)–(d) show the average kernel-level latency involved in the attention operation. The latency for scoring each KV page ( $\text{score}(Q)$ ) and top- $k$  selection remain unchanged from Quest to RetroAt-

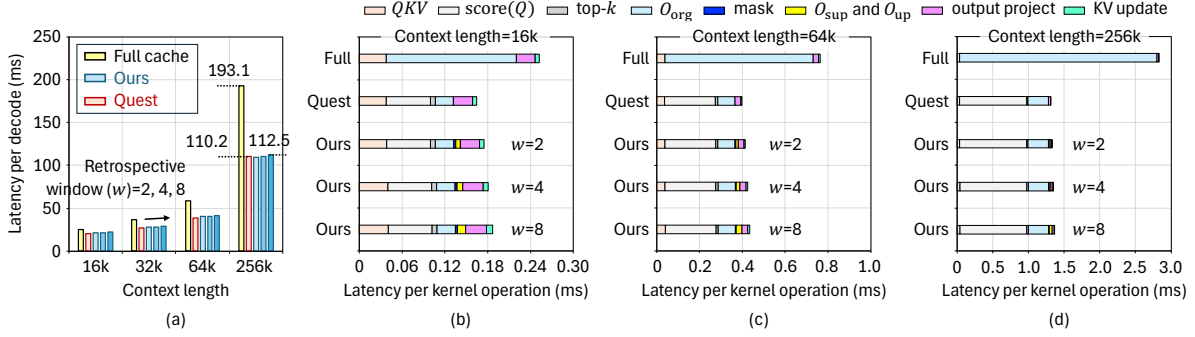


Figure 6: **Latency analysis.** (a) Comparison of end-to-end latency per decoding between full cache (no compression), Quest, and ours with three retrospective window sizes. (b)-(d) Comparison of kernel-level latency breakdown between full cache (denoted as Full), Quest, and ours with three context lengths. Latency results are estimated and then averaged in the 1024 decoding steps followed by prefill with context length. We set the relative budget (b) to 0.15.

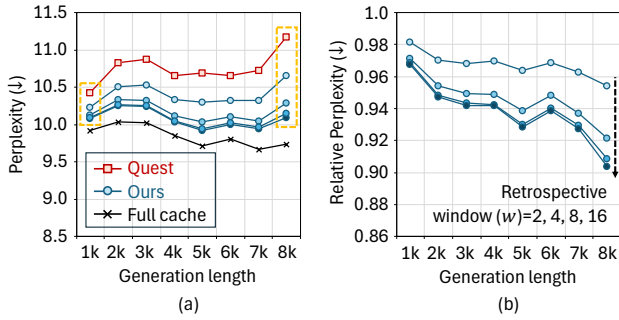


Figure 7: **Comparison in language modeling.** The average perplexity results of the full-cache baseline, Quest, and ours in PG-19 are compared across generation lengths (given 8k prefill length). Initial 8k tokens are processed with full attention (prefill), followed by 8k sparse decoding steps. Relative perplexity denotes a ratio between Quest’s and ours perplexity. We set  $b$  to 0.15.

tention, as they operate only on the most recent Query. Additional operations introduced by RetroAttention—such as projecting historical Queries and Keys, overwriting the KV cache, managing masks, and merging attention outputs—incur overhead. However, these costs are small and largely constant across context lengths, making their relative impact increasingly negligible as the context grows.

## 4.2 Comparison in other Tasks

**Language Modeling.** Fig. 7 presents the comparison of perplexity in PG-19 measured with 1k-token intervals during decoding. Our method consistently reduces perplexity across all intervals compared to Quest (Fig. 7(b)), particularly effective in later generation. This explicitly verifies that the retrospective updates consistently improve output logits across varying window sizes ( $w$ ) as well. We note that the gains saturate beyond  $w=8$ , implying the upper bound in RetroAttention’s performance improvement.

Table 2: **Comparison in reasoning-intensive tasks.** Accuracy results on AIME 2024, GPQA-DIAMOND and LIVECODEBENCH-v5 datasets are summarized with four retrospective window sizes. We set  $b$  and  $w$  to 0.15 and 2.

Method / Benchmark	AIME24 Pass@1 (↑)	GPQA-D Pass@1 (↑)	LCBv5 Pass@1 (↑)
Full Attention	47.1	38.9	37.6
StreamingLLM	0.4	19.7	1.5
TOVA	0.4	0.0	7.0
Quest	<u>33.8</u>	<u>33.6</u>	<u>32.7</u>
<b>RetroAttention (Ours)</b>	<b>39.2</b>	<b>33.6</b>	<b>34.1</b>
$\Delta$ Ours - Quest	+5.4	0.0	+1.4

**Reasoning Tasks.** Tab. 2 presents accuracy results on AIME 2024, GPQA-DIAMOND, and LIVECODEBENCH-v5. Similarly in LONGGENBENCH, the eviction-based methods suffer large degradation compared with full attention; for example, TOVA often fails to follow instructed format during decoding in GPQA-DIAMOND. While RetroAttention exhibits similar accuracy in GPQA-D, significant gains over Quest are observed in the others.

## 5 Conclusion

We introduce RetroAttention, a lightweight yet effective KV cache compression technique, for mitigating cumulative attention errors in long-context generation. Our approach fundamentally differs from conventional sparse attention. Previous methods treat attention outputs as fixed—once computed, the loaded KV entries are discarded and errors persist through the model. RetroAttention instead reuses those KV entries to retrospectively revise past outputs and overwrite stale KV states, enabling consistent correction of cumulative attention errors—without increasing KV cache budget. This design yields consistent accuracy improvements in long-context generation, while maintaining negligible memory and latency overhead.

## References

- Adnan, M.; Arunkumar, A.; Jain, G.; Nair, P. J.; Soloveychik, I.; and Kamath, P. 2024. Keyformer: Kv cache reduction through key tokens selection for efficient generative inference. *Proceedings of Machine Learning and Systems*, 6: 114–127.
- Cai, Z.; Zhang, Y.; Gao, B.; Liu, Y.; Li, Y.; Liu, T.; Lu, K.; Xiong, W.; Dong, Y.; Hu, J.; et al. 2024. Pyramidkv: Dynamic kv cache compression based on pyramidal information funneling. *arXiv preprint arXiv:2406.02069*.
- Chen, M.; Tworek, J.; Jun, H.; Yuan, Q.; Pinto, H. P. D. O.; Kaplan, J.; Edwards, H.; Burda, Y.; Joseph, N.; Brockman, G.; et al. 2021. Evaluating large language models trained on code. *arXiv preprint arXiv:2107.03374*.
- Chen, R.; Wang, Z.; Cao, B.; Wu, T.; Zheng, S.; Li, X.; Wei, X.; Yan, S.; Li, M.; and Liang, Y. 2024a. Arkvale: Efficient generative llm inference with recallable key-value eviction. *Advances in Neural Information Processing Systems*, 37: 113134–113155.
- Chen, Z.; Sadhukhan, R.; Ye, Z.; Zhou, Y.; Zhang, J.; Nolte, N.; Tian, Y.; Douze, M.; Bottou, L.; Jia, Z.; et al. 2024b. Magicpig: Lsh sampling for efficient llm generation. *arXiv preprint arXiv:2410.16179*.
- Cobbe, K.; Kosaraju, V.; Bavarian, M.; Chen, M.; Jun, H.; Kaiser, L.; Plappert, M.; Tworek, J.; Hilton, J.; Nakano, R.; Hesse, C.; and Schulman, J. 2021. Training Verifiers to Solve Math Word Problems. *arXiv preprint arXiv:2110.14168*.
- Comanici, G.; Bieber, E.; Schaekermann, M.; Pasupat, I.; Sachdeva, N.; Dhillon, I.; Blistein, M.; Ram, O.; Zhang, D.; Rosen, E.; et al. 2025. Gemini 2.5: Pushing the Frontier with Advanced Reasoning, Multimodality, Long Context, and Next Generation Agentic Capabilities. *arXiv preprint arXiv:2507.06261*.
- Dai, J.; Huang, Z.; Jiang, H.; Chen, C.; Cai, D.; Bi, W.; and Shi, S. 2024. CORM: Cache Optimization with Recent Message for Large Language Model Inference. *arXiv preprint arXiv:2404.15949*.
- Dao, T.; Fu, D.; Ermon, S.; Rudra, A.; and Ré, C. 2022. Flashattention: Fast and memory-efficient exact attention with io-awareness. *Advances in neural information processing systems*, 35: 16344–16359.
- Fu, Y. 2024. Challenges in deploying long-context transformers: A theoretical peak performance analysis. *arXiv preprint arXiv:2405.08944*.
- Ge, S.; Zhang, Y.; Liu, L.; Zhang, M.; Han, J.; and Gao, J. 2023. Model tells you what to discard: Adaptive kv cache compression for llms. *arXiv preprint arXiv:2310.01801*.
- Guo, D.; Yang, D.; Zhang, H.; Song, J.; Zhang, R.; Xu, R.; Zhu, Q.; Ma, S.; Wang, P.; Bi, X.; et al. 2025. Deepseek-r1: Incentivizing reasoning capability in llms via reinforcement learning. *arXiv preprint arXiv:2501.12948*.
- Hendrycks, D.; Burns, C.; Basart, S.; Zou, A.; Mazeika, M.; Song, D.; and Steinhardt, J. 2021. Measuring Massive Multitask Language Understanding. *Proceedings of the International Conference on Learning Representations (ICLR)*.
- Hooper, C.; Kim, S.; Mohammadzadeh, H.; Maheswaran, M.; Paik, J.; Mahoney, M. W.; Keutzer, K.; and Gholami, A. 2024. Squeezed attention: Accelerating long context length llm inference. *arXiv preprint arXiv:2411.09688*.
- Jaech, A.; Kalai, A.; Lerer, A.; Richardson, A.; El-Kishky, A.; Low, A.; Helyar, A.; Madry, A.; Beutel, A.; Carney, A.; et al. 2024. Openai o1 system card. *arXiv preprint arXiv:2412.16720*.
- Jain, N.; Han, K.; Gu, A.; Li, W.-D.; Yan, F.; Zhang, T.; Wang, S.; Solar-Lezama, A.; Sen, K.; and Stoica, I. 2024. Livecodebench: Holistic and contamination free evaluation of large language models for code. *arXiv preprint arXiv:2403.07974*.
- Jiang, J.; Wang, F.; Shen, J.; Kim, S.; and Kim, S. 2024. A survey on large language models for code generation. *arXiv preprint arXiv:2406.00515*.
- Kwon, W.; Li, Z.; Zhuang, S.; Sheng, Y.; Zheng, L.; Yu, C. H.; Gonzalez, J.; Zhang, H.; and Stoica, I. 2023. Efficient memory management for large language model serving with pagedattention. In *Proceedings of the 29th symposium on operating systems principles*, 611–626.
- Li, Y.; Huang, Y.; Yang, B.; Venkitesh, B.; Locatelli, A.; Ye, H.; Cai, T.; Lewis, P.; and Chen, D. 2024. Snapkv: Llm knows what you are looking for before generation. *Advances in Neural Information Processing Systems*, 37: 22947–22970.
- Liu, D.; Chen, M.; Lu, B.; Jiang, H.; Han, Z.; Zhang, Q.; Chen, Q.; Zhang, C.; Ding, B.; Zhang, K.; et al. 2024a. Retrievalattention: Accelerating long-context llm inference via vector retrieval. *arXiv preprint arXiv:2409.10516*.
- Liu, G.; Li, C.; Zhao, J.; Zhang, C.; and Guo, M. 2024b. Clusterkv: Manipulating llm kv cache in semantic space for recallable compression. *arXiv preprint arXiv:2412.03213*.
- Liu, X.; Dong, P.; Hu, X.; and Chu, X. 2024c. Longgenbench: Long-context generation benchmark. *arXiv preprint arXiv:2410.04199*.
- Liu, Z.; Desai, A.; Liao, F.; Wang, W.; Xie, V.; Xu, Z.; Kyrillidis, A.; and Shrivastava, A. 2023. Scissorhands: Exploiting the persistence of importance hypothesis for llm kv cache compression at test time. *Advances in Neural Information Processing Systems*, 36: 52342–52364.
- Oren, M.; Hassid, M.; Yarden, N.; Adi, Y.; and Schwartz, R. 2024. Transformers are multi-state rnns. *arXiv preprint arXiv:2401.06104*.
- Rae, J. W.; Potapenko, A.; Jayakumar, S. M.; Hillier, C.; and Lillicrap, T. P. 2019. Compressive Transformers for Long-Range Sequence Modelling. *arXiv preprint*.
- Rein, D.; Hou, B. L.; Stickland, A. C.; Petty, J.; Pang, R. Y.; Dirani, J.; Michael, J.; and Bowman, S. R. 2024. Gpqa: A graduate-level google-proof q&a benchmark. In *First Conference on Language Modeling*.
- Ribar, L.; Chelombiev, I.; Hudlass-Galley, L.; Blake, C.; Luschi, C.; and Orr, D. 2023. Sparq attention: Bandwidth-efficient llm inference. *arXiv preprint arXiv:2312.04985*.
- Singhania, P.; Singh, S.; He, S.; Feizi, S.; and Bhatele, A. 2024. Loki: Low-rank keys for efficient sparse attention.



*Advances in Neural Information Processing Systems*, 37: 16692–16723.

Song, J.; Jo, D.; Kim, Y.; and Kim, J.-J. 2025. Reasoning Path Compression: Compressing Generation Trajectories for Efficient LLM Reasoning. *arXiv preprint arXiv:2505.13866*.

Sun, Y.; Ye, T.; Dong, L.; Xia, Y.; Chen, J.; Gao, Y.; Cao, S.; Wang, J.; and Wei, F. 2025. Rectified Sparse Attention. *arXiv preprint arXiv:2506.04108*.

Talmor, A.; Herzig, J.; Lourie, N.; and Berant, J. 2019. CommonsenseQA: A Question Answering Challenge Targeting Commonsense Knowledge. In *Proceedings of the 2019 Conference of the North American Chapter of the Association for Computational Linguistics: Human Language Technologies, Volume 1 (Long and Short Papers)*, 4149–4158. Minneapolis, Minnesota: Association for Computational Linguistics.

Tang, J.; Zhao, Y.; Zhu, K.; Xiao, G.; Kasikci, B.; and Han, S. 2024. Quest: Query-aware sparsity for efficient long-context llm inference. *arXiv preprint arXiv:2406.10774*.

Wu, W.; Pan, Z.; Wang, C.; Chen, L.; Bai, Y.; Wang, T.; Fu, K.; Wang, Z.; and Xiong, H. 2024. Tokenselect: Efficient long-context inference and length extrapolation for llms via dynamic token-level kv cache selection. *arXiv preprint arXiv:2411.02886*.

Xiao, C.; Zhang, P.; Han, X.; Xiao, G.; Lin, Y.; Zhang, Z.; Liu, Z.; and Sun, M. 2024. Inllm: Training-free long-context extrapolation for llms with an efficient context memory. *arXiv preprint arXiv:2402.04617*.

Xiao, G.; Tian, Y.; Chen, B.; Han, S.; and Lewis, M. 2023. Efficient Streaming Language Models with Attention Sinks. *arXiv*.

Yang, S.; Sheng, Y.; Gonzalez, J. E.; Stoica, I.; and Zheng, L. 2024. Post-training sparse attention with double sparsity. *arXiv preprint arXiv:2408.07092*.

Ye, Z.; Chen, L.; Lai, R.; Lin, W.; Zhang, Y.; Wang, S.; Chen, T.; Kasikci, B.; Grover, V.; Krishnamurthy, A.; et al. 2025. Flashinfer: Efficient and customizable attention engine for llm inference serving. *arXiv preprint arXiv:2501.01005*.

Yi, Z.; Ouyang, J.; Liu, Y.; Liao, T.; Xu, Z.; and Shen, Y. 2024. A survey on recent advances in llm-based multi-turn dialogue systems. *arXiv preprint arXiv:2402.18013*.

Yuan, Z.; Shang, Y.; Zhou, Y.; Dong, Z.; Zhou, Z.; Xue, C.; Wu, B.; Li, Z.; Gu, Q.; Lee, Y. J.; et al. 2024. Llm inference unveiled: Survey and roofline model insights. *arXiv preprint arXiv:2402.16363*.

Zadouri, T.; Strauss, H.; and Dao, T. 2025. Hardware-efficient attention for fast decoding. *arXiv preprint arXiv:2505.21487*.

Zhang, Z.; Sheng, Y.; Zhou, T.; Chen, T.; Zheng, L.; Cai, R.; Song, Z.; Tian, Y.; Ré, C.; Barrett, C.; et al. 2023. H2o: Heavy-hitter oracle for efficient generative inference of large language models. *Advances in Neural Information Processing Systems*, 36: 34661–34710.

Zhu, K.; Gao, Y.; Zhao, Y.; Zhao, L.; Zuo, G.; Gu, Y.; Xie, D.; Ye, Z.; Kamahori, K.; Lin, C.-Y.; et al. 2025. {NanoFlow}: Towards Optimal Large Language Model Serving Throughput. In *19th USENIX Symposium on Operating Systems Design and Implementation (OSDI 25)*, 749–765.

**Overview.** This appendix provides supplementary material for our manuscript, “Retrospective Sparse Attention for Efficient Long-Context Generation.” It includes additional implementation details and theoretical analysis that complement Sec. 3 of the main article, and provides detailed descriptions of the experimental settings. Sec. A describes additional implementation details of the main RetroAttention algorithm, including attention output updates and the retrospective mask logic. In Sec. B, extending the discussion in Sec. 3.5 of the main paper, we elaborate on the overhead analysis for linear layers, showing that the additional latency remains negligible due to their memory-bound nature. In addition to the memory traffic discussion in Sec. 3.5, Sec. C quantifies RetroAttention’s memory footprint. Lastly, Sec. D outlines dataset statistics, prompt formats, and experimental configurations for our latency and accuracy evaluations.

## A Implementation Details

**RetroAttention Algorithm Flow.** Alg. 1 presents the detailed logic of RetroAttention. Lines 2, 5, 7, and 8 shows the additional operations introduced by RetroAttention: updating previous KV caches, updating the attended mask cache and building masks for the attention kernel, merging cached and current partial outputs, and caching current outputs. The attention operation (Line 6) processes  $w$  Queries instead of a single Query. As our method is not constrained by a specific top- $k$  page selection method (*e.g.*, Quest), we can integrate RetroAttention into any non-eviction dynamic sparse attention methods. To efficiently support these additional operations, we implement custom CUDA kernels—for page masking (Line 2) and incremental updates (Line 7)—and modify the main attention kernel to handle custom attention masking. We also extend the KV cache append kernel to support updates. Our modified attention kernel builds on Flash-Infer (Ye et al. 2025), a high-performance attention computation framework.

**Updated Attention Output.** As discussed in Sec. 3.3 (main), the updated attention output  $O_{\text{up}, t}$  is computed by a weighted linear combination of the original and supplementary attention outputs. Let us rewrite  $O_{\text{org}, t}$  and  $O_{\text{sup}, t}$  in Eqs. 2 and 3 (main) with explicit superscripts to clarify which decoding step each tensor comes from as follows:

$$O_{\text{org}, t} = \frac{\sum_{j \in S_t} \sum_{l \in \text{Page}_j} e^{Q_t^t K_l^{t\top} / \sqrt{d}} V_l^t}{\sum_{i \in S_t} \sum_{l \in \text{Page}_i} e^{Q_t^t K_l^{t\top} / \sqrt{d}}} \quad (7)$$

$$O_{\text{sup}, t}^{t+s} = \frac{\sum_{j \in S_{t+s} \setminus \bigcup_{m=t}^{t+s-1} S_m} \sum_{l \in \text{Page}_j} e^{Q_t^{t+s} K_l^{t+s\top} / \sqrt{d}} V_l^{t+s}}{\sum_{i \in S_{t+s} \setminus \bigcup_{m=t}^{t+s-1} S_m} \sum_{l \in \text{Page}_i} e^{Q_t^{t+s} K_l^{t+s\top} / \sqrt{d}}} \quad (8)$$

where the superscripts  $t$  and  $t+s$  indicate the decoding step in which the tensor ( $QKV$ ) was computed and the subscript  $t$  indicates its corresponding token index. As discussed in Sec. 3.4, retrospective updates to the hidden states of previous tokens propagate to subsequent layers, where the

---

### Algorithm 1: RETROATTENTION

---

**Input:** page selector PAGESELECT; queries  $Q_{i:t}$ , keys  $K_{i:t}$ , values  $V_{i:t}$ ; K/V cache  $C$ ; cached output  $\hat{O}_{i:t-1}$ ; cached attention-lse  $\hat{Z}_{i:t-1}$ ; window size  $w$

**Output:** outputs  $O_{i:t}$ ; updated cache  $C$

```

1  $i \leftarrow t - w + 1$ ; // Window start index
2 UpdateKV( $K_{i:t-1}, V_{i:t-1}, C$ );
3 AppendKV( $K_t, V_t, C$ );
4  $S_t \leftarrow \text{PAGESELECT}(Q_t, C)$ ;
5  $M \leftarrow \text{UpdateAndBuildMask}(S_t, C)$ ;
6  $(O_{i:t}, Z_{i:t}) \leftarrow \text{Attention}(Q_{i:t}, S_t, M, C)$ ;
7  $(O_{i:t-1}, Z_{i:t-1}) \leftarrow$ 
   MergeOutput( $\hat{O}_{i:t-1}, \hat{Z}_{i:t-1}, O_{i:t-1}, Z_{i:t-1}$ );
8 CacheOutput( $O_{\max(i, t-w+2):t}, Z_{\max(i, t-w+2):t}, C$ );
9 return  $O_{i:t}, C$ 
```

---

corresponding  $QKV$  vectors are also updated. Therefore, it is necessary to distinguish  $QKV$  vectors for the same token index using superscripts that indicate the time at which they were computed. For example,  $Q_t$  is generated at the decoding step  $t$  for the first time, but at  $t+s$ , the updated attention outputs from the previous layer provide new embeddings to the current layer and then generates another  $Q_t$  (omitted in green line in Fig. 4 (main)). To distinguish these two  $Q_t$ s, we denote the first  $Q_t$  generated at  $t$  as  $Q_t^t$  and the second  $Q_t$  generated at  $t+s$  as  $Q_t^{t+s}$ .

As the first supplementary attention becomes available at step  $t+1$  (*i.e.*,  $s=1$ ), RetroAttention merges  $O_{\text{org}, t}$  and  $O_{\text{sup}, t}^{t+1}$  by a weighted average whose coefficients are the respective softmax normalizers:

$$\begin{aligned}
O_{\text{up}, t}^{t+1} &= \frac{\alpha_{\text{org}} \cdot O_{\text{org}, t} + \alpha_{\text{sup}}^{t+1} \cdot O_{\text{sup}, t}^{t+1}}{\alpha_{\text{org}} + \alpha_{\text{sup}}^{t+1}} \\
\alpha_{\text{up}}^{t+1} &= \alpha_{\text{org}} + \alpha_{\text{sup}}^{t+1} \\
\alpha_{\text{org}} &= \sum_{i \in S_t} \sum_{j \in \text{Page}_i} e^{Q_t^t K_j^{t\top} / \sqrt{d}} \\
\alpha_{\text{sup}}^{t+1} &= \sum_{i \in S_{t+1} \setminus S_t} \sum_{j \in \text{Page}_i} e^{Q_t^{t+1} K_j^{t+1\top} / \sqrt{d}}
\end{aligned} \quad (9)$$

This procedure is applied recursively as additional supplementary outputs arrive—that is,  $O_{\text{sup}, t}^{t+2}$  and  $O_{\text{up}, t}^{t+1}$  are merged through  $\alpha_{\text{sup}}^{t+2}$  and  $\alpha_{\text{up}}^{t+1}$  by the same mechanism:

$$\begin{aligned}
O_{\text{up}, t}^{t+s+1} &= \frac{\alpha_{\text{up}}^{t+s} \cdot O_{\text{up}, t}^{t+s} + \alpha_{\text{sup}}^{t+s+1} \cdot O_{\text{sup}, t}^{t+s+1}}{\alpha_{\text{up}}^{t+s} + \alpha_{\text{sup}}^{t+s+1}} \\
\alpha_{\text{up}}^{t+s+1} &= \alpha_{\text{up}}^{t+s} + \alpha_{\text{sup}}^{t+s+1} \\
\alpha_{\text{sup}}^{t+s+1} &= \sum_{i \in S_{t+s+1} \setminus \bigcup_{r=0}^s S_{t+r}} \sum_{j \in \text{Page}_i} e^{Q_t^{t+s+1} K_j^{t+s+1\top} / \sqrt{d}}
\end{aligned} \quad (10)$$

**Evolving Query Representations in Past Attention.** As discussed in the above paragraph, the updated attention output is transferred to the next layer and then projected into a

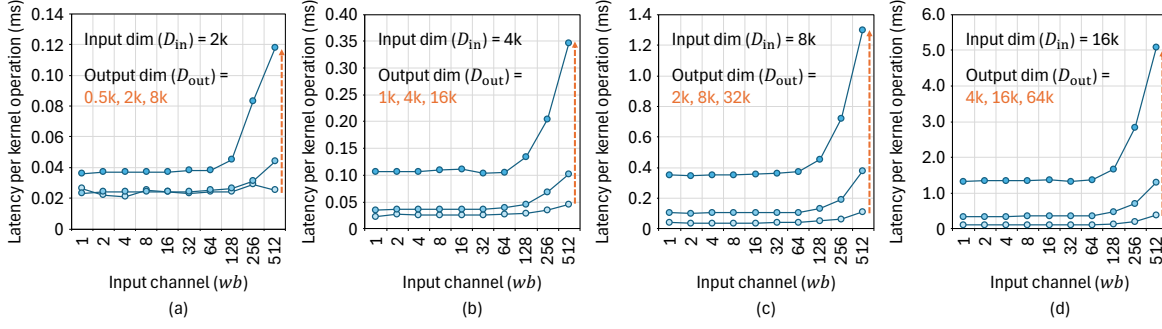


Figure 8: **Latency analysis for linear layers.** Kernel latency of RetroAttention in a linear layer with various input and output dimensions (denoted in the figure) and input channel sizes. For RetroAttention, the input channel size equals  $w \times b$ , where  $w$  is the retrospective window size and  $b$  is the batch size.

---

**Algorithm 2:** UPDATEANDBUILDMASK (Single Head)

---

**Input:** page index list  $S_t$ ; cache  $\mathcal{A}$ ; last page index

$p_{\text{curr}}$

**Output:** attention mask  $M$ ; updated cache  $\mathcal{A}$

- 1  $\mathcal{A}[p_{\text{curr}}] \leftarrow t - 1$ ; // Prevent current page from being attended by previous queries
  - 2  $M \leftarrow []$ ;
  - 3 **foreach**  $p \in S_t$  **do**
  - 4      $M.append(\mathcal{A}[p])$ ;
  - 5      $\mathcal{A}[p] \leftarrow t$ ;
  - 6 **end**
  - 7 **return**  $M, \mathcal{A}$
- 

new Query representation. This implies that Query representation at a given layer evolve as the update repeats. Dao et al. (2022) analytically show that the aggregation of two partial softmax outputs can be exactly same as the original softmax output. This assumes the partial outputs are generated at the same decoding steps (*i.e.*, based on the same Query representation), whereas RetroAttention merges the attention output asynchronously generated across a retrospective window. This leads to a mismatch in Query representations due to their evolution during retrospective updates.

Our updated attention output, merging multiple outputs across a retrospective window, is an approximation of the attention output on the total supplemented KV entries that would have been computed as normal sparse attention. We assume that the  $QKV$  representations evolve smoothly across decoding steps, such that those from consecutive steps can be regarded as approximately equivalent. Empirically, the  $\ell_2$  distance between the same vector across adjacent steps (*i.e.*, the change induced by one retrospective update) is typically less than 5% of its original  $\ell_2$  norm for Query and Key vectors on average across various tasks, and less than 10% for Value vectors.

**Retrospective Mask.** The supplementary attention outputs are computed only on unseen KV cache pages. We in-

troduce a *retrospective mask* ( $\mathcal{A}$ ) to identify which pages have been already attended before and avoid their duplicated updates. Specifically, for each page  $p$ , we store  $\mathcal{A}_h[p]$ , the last decoding step in which the page was loaded for a head  $h$ . This indicates that the attention outputs preceding the  $\mathcal{A}_h[p]$ -th decoding step are already supplemented with the page  $p$ , if unseen. Accordingly, when computing the supplementary attention for the past (*e.g.*, decoding step  $t$ ) Query and head  $h$ , we mask out any page  $p$  such that  $\mathcal{A}_h[p] \geq t$ . Let  $k_{\text{page}}$  be the number of loaded pages,  $\mathcal{P}$  the global page pool (*i.e.*, the entire KV cache),  $L$  the sequence length, and  $P$  the page size. This incremental masking logic relies only on tracking the latest Query per page, requiring  $h_k |\mathcal{P}| = h_k L/P$  integers per layer for tracking and  $h_k k_{\text{page}}$  integers to be loaded per kernel call, assuming  $h_k$ -wise page selection. Alg. 2 describe the detailed mask management logic.

## B Linear Layer Overhead Analysis

For an input of shape  $n \times D_{\text{in}}$  and a projection weight of shape  $D_{\text{in}} \times D_{\text{out}}$ , the arithmetic intensity (AI) of linear layers in FP16 precision is given:

$$\text{AI}_{\text{linear}} = \frac{nD_{\text{in}}D_{\text{out}}}{nD_{\text{in}} + D_{\text{in}}D_{\text{out}} + nD_{\text{out}}} \quad (11)$$

where  $n$  is batch  $\times$  sequence length. This shows that when  $n \ll D_{\text{out}}$  (which is typical in decoding stage), the AI becomes small, indicating that the operation is *memory-bound* rather than *compute-bound*. This allows models to have capacity for more computation with only negligible latency overhead. Fig. 8 shows that the linear layer latency remains nearly constant until  $n$  exceeds a certain threshold in diverse  $D_{\text{in}}$  and  $D_{\text{out}}$  combinations. These observations validate that the overhead per decoding step introduced by RetroAttention—whose linear layers process  $w$  times larger input per step (*i.e.*,  $n$  is  $w \times \text{batch}$ )—is practically negligible unless  $n$  is around 128-256. Moreover, this overhead is independent of sequence length and the number of loaded KV entries, making it suitable for long generation scenarios.

Table 3: LONGGENBENCH Prompt Template

Prompt Template
<p>Answer each question step by step, adhering to the format shown in the examples provided. Start each response with ‘Answer’ and introduce the final response with ‘The answer is’. Do not repeat the question. Ensure that you respond to all the questions presented, regardless of their number.</p> <p><b>Examples:</b></p> <p>{CoT Question_1} ... {CoT Question_k}</p> <p>{CoT Answer_1} ... {CoT Answer_k}</p> <p><b>Following Question:</b></p> <p>{Real Question_1} ... {Real Question_n}</p>

## C Memory Footprint Analysis

Memory footprint is another critical factor to consider—especially since KV cache occupancy dominates attention memory usage and constrains inference concurrency in scenarios such as offloading (Fu 2024). It is therefore important to analyze the peak memory consumption during decoding, which typically arises from the attention operation due to the large KV cache it requires. Following the same notation in Sec. 3.5 (*e.g.*, the retrospective window size  $w$ , number of loaded KV pages  $k_{\text{page}}$ , Query heads  $h_q$ , tokens per page  $P$ , and head dimension  $d$ ), the memory required for the caches involved in sparse attention computation is

$$2 k_{\text{page}} P h_k d B \text{ bytes} \quad (12)$$

RetroAttention adds only small memory overhead by storing the attention outputs from the previous  $w-1$  steps:

$$(w-1) h_q (d+2) B \quad (13)$$

bytes, including auxiliary FP32 log-sum-exp values. This term is independent of both  $k_{\text{page}}$  and sequence length  $L$ , making its growth negligible relative to the generation length. In addition, the masking mechanism, which records the most recent decoding step for each KV page per head, requires

$$h_k \left( \frac{L}{P} \right) \cdot 2B \quad (14)$$

bytes (assuming 32-bit integers). Overall, these additions incur minimal memory overhead compared to the KV cache and do not affect scalability.

## D Dataset and Experiment Details

**Dataset.** We primarily evaluate on LONGGENBENCH, which constructs a single input prompt by concatenating multiple reasoning questions in sequence. Tab. 3 displays a prompt template used for LONGGENBENCH evaluation. We follow the original implementation for the number of in-context examples ( $k$ ) (Liu et al. 2024c). Note that this differs with the number of concatenated examples in a prompt ( $n$ ). Also, Tab. 4 reports the input and output token statistics for the three datasets in LONGGENBENCH: CSQA, GSM8K, and MMLU. The number of input and output tokens grows almost linearly with the number of questions in a prompt. Reasoning-intensive benchmarks, AIME 2024,

Table 4: **Data statistics in LONGGENBENCH.** Input and Output Tokens denote the average number of input tokens and output (generated from full-cache model) tokens.

Benchmark	$n$ -question	Input Tokens	Output Tokens
CSQA	15	1337.9	657.8
	30	2029.8	1327.3
	45	2672.3	1964.6
GSM8K	15	1705.8	1495.0
	30	2649.7	2956.8
	45	3530.6	4238.1
MMLU	15	2615.7	951.6
	30	4200.8	1637.2
	45	5744.3	2427.5

GPQA-DIAMOND, and LIVECODEBENCH-v5, are evaluated using nucleus sampling (temperature 0.6; top- $p$  0.95) with 8, 2, and 1 samples per question, respectively. Language modeling benchmark, PG-19 is evaluated on 91 out of 100 test samples exceeding 16k tokens, using the first 16k tokens of each.

**Latency Evaluation.** We evaluate the latency per decoding in end-to-end and kernel breakdown manner at several context lengths. For experimental details, we set the batch size to 8 and relative budget to 0.15, and use a NVIDIA A100 80G GPU. Our kernel implementation is based on FlashInfer (Ye et al. 2025), extensively optimizing CPU-side overheads such as scheduling, synchronization, and memory allocation.

Fig. 6(b)–(d) presents the kernel-level latency breakdown. The segments labeled  $QKV$  and *output project* denote the linear projections from input hidden states to Queries, Keys, and Values, and from the attention outputs to the final projected representations, respectively.  $\text{score}(Q)$  corresponds to the criticality estimation step (Tang et al. 2024), where each page is scored using Quest’s page digests. The *top-k* kernel indicates the selection of the highest-scoring  $k$  pages, while *mask* represents the construction and update of the attention mask, as detailed in Alg. 2. The terms  $O_{\text{org}}$  and  $O_{\text{sup}}/O_{\text{up}}$  account for two separate kernel executions: the attention output computation and the subsequent merging of cached and supplementary outputs when required. Here,  $O_{\text{org}}$  denotes the attention operation time without RetroAttention, while the additional cost introduced by RetroAttention is given by the difference between the combined kernel time and  $O_{\text{org}}$ , denoted as  $O_{\text{sup}}/O_{\text{up}}$ . This term reflects the net overhead incurred in attention output computation. Finally, *KV update* reflects the cost of appending and maintaining the key-value caches.